Transportation Research Part D 142 (2025) 104710

Contents lists available at ScienceDirect

Transportation Research Part D

journal homepage: www.elsevier.com/locate/trd

The effect of using N1% as input for aircraft noise modelling

Rebekka C. van der Grift *, Mirjam Snellen, Alireza Amiri-Simkooei

Faculty of Aerospace Engineering, Section Aircraft Noise and Climate Effects, Delft University of Technology, The Netherlands

ARTICLE INFO

Keywords:
Doc.29 aircraft noise model
N1% estimation
Thrust estimation
Aircraft condition monitoring system (ACMS)

ABSTRACT

For models that evaluate aircraft noise, thrust is an essential input. From aircraft flight recorder data or measured noise spectra, the engine's rotational speed can be estimated for which a conversion is then needed to obtain the engine's thrust. This research investigates three conversion methods. The first uses the expressions from the ANP database while the second method is based on the fuel flow. The third employs Gas Turbine Simulation Program (GSP) predictions. The thrust estimates are compared to airline performance calculations where significant variations up to 3 dBA in predicted noise were found. Methods one and three were found to be in good agreement with the performance data. An important finding of this paper is that combining methods one and three using least-squares is capable of providing the required conversion expressions, in line with those in the ANP database, but without being limited to a few aircraft types only.

1. Introduction

Aircraft noise significantly affects the health and sleep of communities surrounding airports (Anna et al., 2013; Basner and McGuire, 2018), making noise reduction a crucial focus for the aviation industry. Efforts to mitigate noise include introducing quieter aircraft and optimizing flight paths to minimize the number of affected individuals. Flight routes are optimized by using aircraft noise models to develop Noise Abatement Procedures (NAP). The most widely used models for these applications are empirical best-practice noise models, such as Doc.29 (European Civil Aviation Conference, 2016b). These models estimate the noise impact in the area around airports for year-round flight operations using Noise-Power-Distance (NPD) tables. As the name suggests, NPD tables provide the expected noise level (in dBA) for combinations of power (engine thrust settings) and the aircraft distance from a ground point. Using a sensitivity analysis, Behere et al. (2020) showed strong correlations between an aircraft's assumed thrust settings and its projected noise impact which underscores the importance of accurate thrust estimation as a key input for noise prediction models.

In best practice, a set of standard departure and arrival procedures is used to model flights which consist of consecutive steps in aircraft altitude and thrust setting. The flight profile is divided into three segments: Initial take-off, cut-back and climb-out. The initial take-off corresponds often to the maximum take-off thrust with a maximum of 25% derated take-off thrust. Once the cut-back altitude is reached, typically around 800 ft for the flights in this study, the aircraft switches to climb thrust and climbs to its designated cruising altitude. These procedural steps are standardized and documented in resources such as the Aircraft Noise and Performance (ANP) database (European Union Aviation Safety Agency, 2024). However, these procedures represent generalized operations and do not capture the unique profiles of individual flights. To design quieter flight procedures and optimize routing, it is essential to represent the actual thrust profiles used during operations accurately. For this purpose, different methods have been developed to estimate thrust from historical flight data.

* Correspondence to: Office 5.06, Kluyverweg 1, 2629HS, Delft, The Netherlands.
E-mail address: r.c.vandergrift@tudelft.nl (R.C. van der Grift).

https://doi.org/10.1016/j.trd.2025.104710
Received 20 December 2024; Received in revised form 18 February 2025; Accepted 11 March 2025
Available online 20 March 2025

Using open-source initiatives such as the OpenSky network (Schäfer et al., 2014), ADS-B (Automatic Dependent Surveillance-Broadcasted) data facilitates more precise performance calculations. Pretto et al. (2022) employs this data source to enhance the estimation of aircraft Take-Off Weights (TOW) and to generate synthetic ANP profiles that more accurately reflect actual flight paths. With the integration of higher resolution data for low-altitude aircraft operations (Pretto et al., 2024), this approach yields improved noise predictions when compared to historical contours and measurements around various airports. Additional performance estimations utilizing the OpenSky network are presented by Sun et al. (2020), which combines engine properties with kinematic and dynamic performance metrics.

A method developed by Struempfel and Hübner (2020) uses ADS-B data combined with Eurocontrols Base of Aircraft Data (BADA) to estimate the weight and thrust of the corresponding aircraft. The BADA fuel consumption model provides coefficients to calculate the aircraft's changing mass along the trajectory and updates its weight to serve as input to the thrust model (Poles, 2009). When using this thrust estimation method instead of the standard procedure, the discrepancies between the model predictions and actual noise measurements were significantly reduced.

An alternative method to estimate aircraft thrust settings involves analysing fan tones from acoustic measurements (Merino-Martínez et al., 2018; Ramseier and Pieren, 2024) or through machine learning algorithms (Meister, 2024). The engine fan operates at a specific rotational speed, measured in rotations per minute (rpm), and is connected to the low-pressure turbine, powered by the low-pressure compressor, or the N1 spool. This fan rotation generates characteristic noise tones, which can be captured through acoustic measurements. This acoustic-based thrust estimation method has demonstrated improved alignment between noise model predictions and measurements. While the sonAIR aircraft noise model (Zellmann et al., 2018; Meister et al., 2021) uses N1 directly as performance input, for best-practice noise models the effectiveness of these thrust estimations heavily relies on the precise conversion of engine rotational speed to thrust.

The same holds when using data from onboard systems such as the Aircraft Condition Monitoring System (ACMS) which logs all operational aspects of the aircraft, including engine settings. The common method for controlling the thrust of a turbo-jet aircraft is by adjusting the earlier mentioned rotational speed N1 (Linke-Diesinger, 2008). The engine thrust is often expressed as a percentage of maximum rotational speed (N1%). In addition to the N1%, the ACMS registers the fuel flow to each engine. However, the actual thrust produced by each engine is not directly recorded. This again, thus requires a conversion of N1% to thrust.

This relation is, however, not trivial. As indicated by Deiler (2023), the relationship between speed, altitude, temperature and N1 to thrust is complex, with all four parameters significantly influencing the thrust output. During the static tests at the end of engine manufacturing, these relations are documented in so-called engine performance manuals (Boeing 747 Performance Engineers Manual, 1989). Unfortunately, this data is often proprietary.

This paper investigates three different methods for estimating aircraft thrust from the engine's rotational speed (N1%) and its impact on noise modelling for departure operations. The goal is to assess the uncertainties inherent in thrust estimation and the validation of these estimates. The first method is the current best-practice approach, utilizing the ANP database. The second method uses data from the ACMS, which relates the N1% parameter to the fuel flow in order to estimate thrust. The third method is a simulation-based approach using the Gas Turbine Simulation Program (GSP) (Nationaal Lucht- en Ruimtevaartlaboratorium, National Aerospace Lab (NLR) GSP Development Team, 2016). These three methods are evaluated by comparing their thrust predictions to those derived from an airline's aircraft performance software. The remaining sections of this paper are organized as follows. A detailed explanation of each method is provided in Section 2. This research is performed on multiple engine and aircraft types to demonstrate how these factors influence the discrepancies between the methods. The resulting thrust estimations and subsequent noise predictions exhibit significant deviations, as discussed in Section 3. In Section 4, a new method is proposed, combining elements of the ANP and GSP approaches to create a more effective and user-friendly model for thrust estimation, eliminating method's one (ANP based) limitation to a few aircraft types only. Finally, in Section 5, the advantages and disadvantages of each method are discussed. Although the validation of thrust input is an underdeveloped aspect of noise modelling, it is an essential step towards accurate aircraft noise predictions. This paper proposes a novel thrust estimation and validation method, aiming at addressing this gap and hence enhancing aircraft noise predictions.

2. Methodology

In best-practice noise models like Doc.29, assumptions on the delivered thrust are made through standard procedures outlined in the ANP database. These models express engine thrust in terms of *corrected net thrust* F_n/δ [lbf] per engine, where δ is the pressure coefficient calculated as the ratio of ambient pressure to mean sea level pressure (p_0 = 101.325 kPa). However, acoustic measurements or flight data typically provide the engine's power setting as its rotational speed (N1%). The N1% is often generalized using the temperature coefficient θ_T to obtain the generalized or corrected N1 (N1%/$\sqrt{\theta_T}$) (European Civil Aviation Conference, 2016a), hereafter just referred to as 'N1%'. The temperature coefficient is the ratio of ambient temperature outside of the engine to the temperature at mean sea level (15 C°) and is used to compensate for the differences in rotational speed in static test conditions on the ground and operational conditions. To find the thrust input for accurate aircraft noise modelling with N1 known, an accurate conversion between N1 and thrust is required. Although during the design and production of engines, every engine manufacturer creates engine-specific performance manuals, they are typically only openly available for outdated engines. Nevertheless, these performance manuals offer valuable insights into engine performance characteristics. One of the key performance characteristics documented in these manuals is the design net thrust versus generalized $N1\%$, where for example, every 0.05 Mach increment, a different curve is given. Examples of such curves for a CF6-80C2 engine are shown in Fig. 1, where $F_n/\delta[\%]$ is the percentage of thrust compared to the maximum flat rated thrust (Boeing 747 Performance Engineers Manual, 1989). It is visible that next to N1%, the Mach number can also significantly influence the thrust produced.

In the remainder of this section, we describe three conversion methods. These methods are tested against airline-provided aircraft performance calculations as described in Section 2.1.

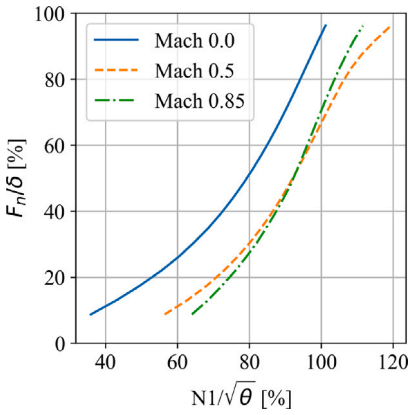

Fig. 1. Relation between generalized $N1\%$ and thrust based on performance manual.

2.1. Data

The different N1-to-Thrust conversion methods will be validated by comparing their predictions with airline-provided aircraft performance calculations. The airline model is, among others, used by pilots to calculate the amount of (derated) take-off thrust required for specific weather and runway conditions. The results of the model are a direct input into the Flight Management System (FMS) and thus depict the actual flown thrust profiles. In addition to local conditions, take-off weight and the degree of thrust derating are crucial inputs for this model.

For this research, airline model simulations were conducted for departure operations for the B737-800 and the B777-200 across a range of take-off weights. The data provided by these models contains, but is not limited to, positional parameters, airspeed, atmospheric conditions, engine parameters (such as N1 and fuel flow) and net corrected thrust per engine. Although this is simulated data, it is of the highest accuracy and quality as it is produced by aircraft manufacturers using advanced performance algorithms. Each simulated flight covers the trajectory from the end of the take-off roll up to an altitude of 3000 m (±9150 ft). The take-off roll is defined from the break release point (BRP) to 35 ft altitude. An example of such a flight is shown in Fig. 2 where the consecutive steps of acceleration and climb are visible.

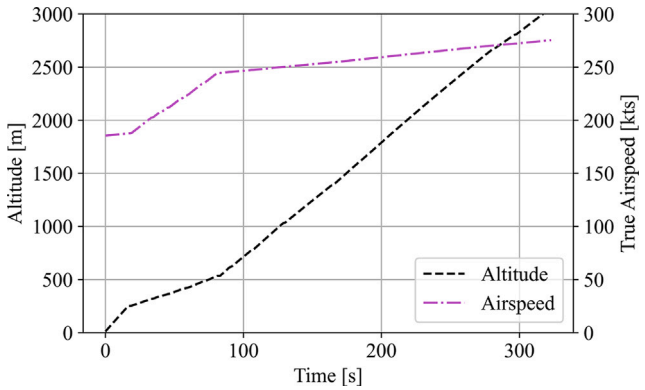

Fig. 2. Altitude and airspeed profile of an B777-200 departure flight from the airline model.

2.2. Method 1: Aircraft noise and performance database

The first method to calculate thrust for noise modelling utilizes the best-practice method provided by the European Civil Aviation Conference (2016a). It is based on engine-specific constants and procedural steps as shown in Table 1. It often assumes specific engine settings for each sequential phase of acceleration and/or climb in a standard procedure in combination with a set of derated thrust levels. Using these inputs, the net thrust is then calculated as

$$\frac{F_n}{\delta} = E_0 + F_0 V_C + G_A h + G_B h^2 + HT, \tag{1}$$

where E_0, F_0, G_A, G_B and H are engine thrust constants chosen per procedural step in units $lb \times s/ft$, lb/ft, lb/ft^2 and $lb/°C$, respectively. These engine thrust constants are calculated during the certification of the aircraft and verified by EASA during

Table 1
ANP coefficients for calculating thrust using standard procedural steps for the B777-200 (European Union Aviation Safety Agency, 2024).

Procedure	E_0	F_0	G_A	G_B	H
MaxClimb	67 093.7	−85.75534	1.8498	−7.60E−05	0
MaxClimbHiTemp	82 096.7	−72.2859	−0.32818	−1.79E−05	−637
MaxTakeoff	93 672.6	−122.25116	1.1818	−8.06E−05	0
MaxTkoffHiTemp	114 758.6	−125.38	−0.159002	−2.61E−05	−702.4

implementation into the ANP database (European Union Aviation Safety Agency, 2024). Further, δ is the pressure coefficient, V_c is the calibrated airspeed in knots, T is the ambient air temperature in Celsius and h is the altitude in*feet*. This equation accounts for the variations in temperature and pressure between the actual and standard atmospheres, and their impact on the engine efficiency.

This method is fast and easy to comprehend but the procedures are often based on assumptions, for example, on the amount and timing of the thrust cutback during departure, or estimates of the aircraft's weight, which affects the required thrust for take-off. The aircraft's TOW is conventionally estimated by the distance to its destination in sets of stage lengths (European Civil Aviation Conference, 2016a), although recent studies include more accurate weight estimations based on flight tracks and performance calculations (Sun et al., 2018; Struempfel and Hübner, 2020; Pretto et al., 2024)

By analysing actual flight tracks, such as those provided by radar data, it is possible to select the most suitable procedures. In Fig. 3, two examples of such cases are shown. In this case, the procedures are matched with flights from the airline model for complementary TOW. It is evident that for a low gross weight, as seen in Fig. 3(a), the thrust is overestimated, while for a high gross TOW, close to the maximum, the thrust is underestimated. For both procedures, the timing of the cutback is offset and the climb thrust patterns differ.

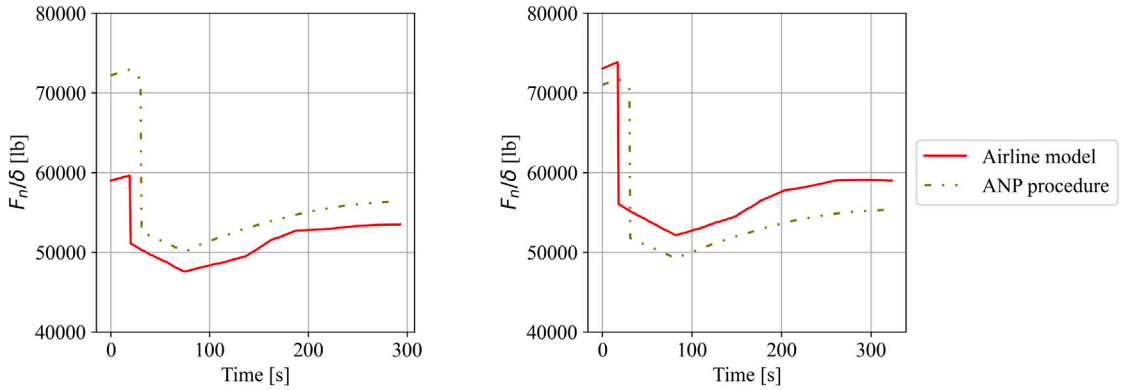

(a) Standard departure procedure of stage length 5 (±3200 nautical miles).

(b) Standard departure procedure of stage length 8 (±6200 nautical miles).

Fig. 3. Airline modelled departure procedures compared with their respective standard ANP procedure for the B777-200.

To avoid part of the above-mentioned assumptions, Eq. (1) can be expanded with the rotational speed $N1\%$ to account for actual flight conditions, as suggested by the (European Civil Aviation Conference, 2016a)

$$\frac{F_n}{\delta} = E_0' + F_0' V_C + G_A' h + G_B' h^2 + H' T + K_3\left(\frac{N1\%}{\sqrt{\theta_T}}\right) + K_4\left(\frac{N1\%}{\sqrt{\theta_T}}\right)^2, \tag{2}$$

where the constants K_3 and K_4 are derived from installed engine data. In this equation, the other engine constants (E_0', F_0', G_A', G_B' and H') are set to their general values, not connected to a specific procedural step, given in the ANP database which differs from the counterparts in Eq. (1), indicated by the primes and depicted in Table 2.

The use of Eq. (2) is straightforward. From the ACMS data or the airline model data, the operational parameters V_C, h and $N1$ can be extracted, along with the atmospheric conditions at the aircraft position. These parameters are required to calculate θ_T and δ. The remaining engine constants can be found in the ANP database. The constant terms K_3 and K_4 are not available for most common aircraft types. Currently, these parameters are only available for the A330-300 and the B777-200. For this reason, these aircraft have been chosen in this research, which excludes most of the commercial aircraft departing and arriving at Schiphol. The parameters are given in Table 2.

An example of the use of this equation in comparison with the airline model can be seen in Fig. 4. Although this method approximates the simulated thrust well, it still overlooks certain effects. For the B777-200, the speed and height parameters F_0' and G' are set to 0. As both airspeed and altitude negatively correlate with thrust, the engine thrust during the acceleration phase decreases (Deiler, 2023). This effect is observed between 20–80 s. The ANP predictions remain constant during this phase, caused

Table 2
ANP coefficients for calculating thrust (European Union Aviation Safety Agency, 2024).

Type	E_0'	F_0'	G_A'	G_B'	H'	K_3	K_4
B777–200	32 710	0	0	0	0	−1258	16.16
A330–300	36 339.3	−31.32	−0.1297	0	0	484.645	4.0056

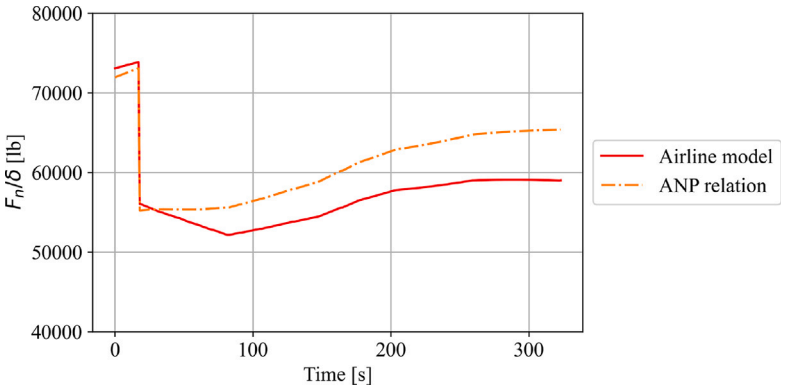

Fig. 4. Airline simulated flight of B777-200 modelled with ANP relation.

by the zero-values of F_0' and G' which results in an overestimation of thrust. After 80 s, when a stable speed is reached and the aircraft climbs further to 3000 m, the overestimation grows due to decreasing atmospheric pressure and temperature, factors that the ANP does not account for.

2.3. Method 2: Fuel flow relation

The previously described method is based on models developed for engine performance. In this paper, a new empirical method is proposed, which uses fuel flow to the engines, $\dot{m}_{ff}$, as gathered from ACMS data and couple this to used N1. Fuel consumption of aircraft engines is directly linked to the requested delivered power (Bensel and Scholz, 2018). This relationship between $\dot{m}_{ff}$ and thrust F_n forms the basis of the proposed method. In contrast to the other methods, this new method is fully based on empirical data obtained by real flight data.

In the ICAO engines emission database, all certified engine types are documented along with their emission characteristics and fuel burn for different stages (European Union Aviation Safety Agency, 2025). These values are documented and tested during the certification of the engines. The tests are static thrust tests on an uninstalled engine in which values such as the fuel flow per Landing and Take-Off (LTO) cycle or the maximum rated thrust are determined. An example of a result is given in Fig. 5(a). It is important to note the distinction between different types of thrust ratings: maximum flat-rated thrust, maximum continuous thrust, and maximum certified thrust. Although the first is often reported, maximum flat-rated thrust is not often used in operation, only in emergencies as it severely decreases engine life.

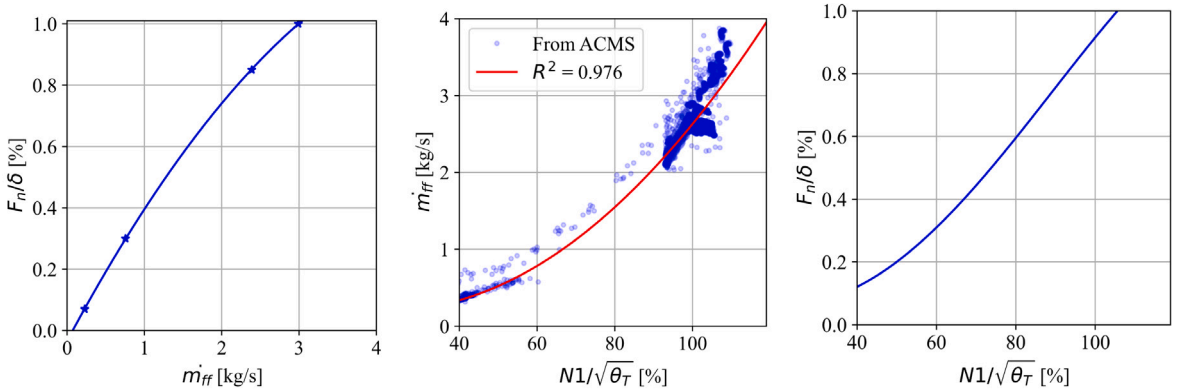

(a) Relation between % of maximum thrust and fuel use from ICAO database.
(b) Fit from ACMS data between fuel-flow and N1%
(c) Found relation between N1% and % of maximum thrust.

Fig. 5. Relations used for determining the N1% to thrust conversion for departures of the A330-300.

The second step in this method is to find a relation between the recorded fuel flow and N1. This is performed by filtering the data of the ACMS for take-off up to 5000 ft and taking all $N1\%$ and recorded fuel flow values for each aircraft type. For the A330-300, a least-squares fit is found to be

$$\dot{m}_{ff}[\mathrm{kg/s}] = 4.497 \times 10^{-4}\left(\frac{N1\%}{\sqrt{\theta_T}}\right)^2 - 2.59 \times 10^{-2}\left(\frac{N1\%}{\sqrt{\theta_T}}\right) + 0.7175 \tag{3}$$

and is visualized as the red fit in Fig. 5(b).

To then couple the ACMS fuel flow to thrust levels, the ACMS reported fuel flow rates at altitude need to be converted to static sea level conditions, as reported in the ICAO database. This is done using Eq. (4) and the Boeing Fuel Flow Method 2 (DuBois and Paynter, 2006).

$$W_{ff} = \frac{\dot{m}_{ff}}{\delta}\left(\theta_T^{3.8} e^{0.2M^2}\right), \tag{4}$$

where M is the mach number and W_{ff} is the corrected fuel flow.

After conversion to ISA sea level conditions, a correction r is applied to account for any installation effects (DuBois and Paynter, 2006). Combining these fuel flow values and the fits indicated in Figs. 5(a) and 5(b), results in a relation between N1 and thrust as illustrated in Fig. 5(c). This final relation between N1 and thrust is specific to this engine type is fully derived from empirical data. For all engine types in this paper, this direct relation between N1 and thrust is found and then used for the performance analysis.

During the analysis, two observations were made. Notably, the ACMS data showed unusually high N1 values, which can likely be attributed to the season in which the data was collected, since the A330-300 dataset is from hot summer days on which the aircraft were likely fully loaded. Furthermore, in all analysed aircraft types, a higher fuel flow was recorded in the ACMS than the maximum of the ICAO database. The values reported in that database are for average emission in the Landing and Take-Off (LTO) cycle, which is only valid below 915 m (3000 ft) (European Union Aviation Safety Agency, 2025). This brings the question of the validity of this engine emission databank for this purpose. In Chati and Balakrishnan (2014), this underestimation of fuel flow in the take-off and climb-out phases was also found and Patterson et al. (2009) found fuel flow rates exceeding the ICAO certifications.

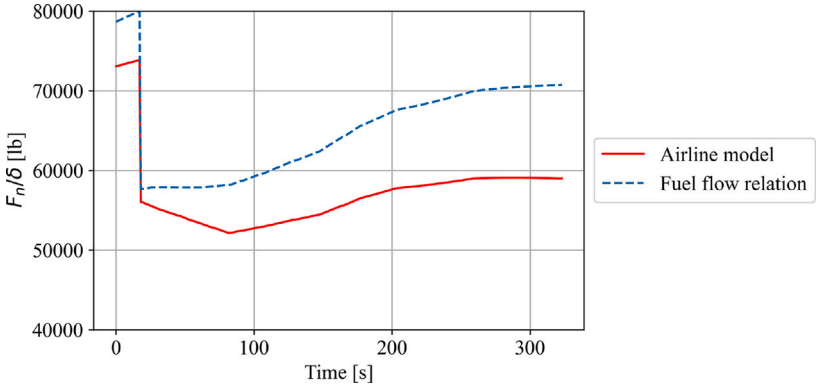

Fig. 6. Airline simulated flight of B777-200 modelled with the derived fuel flow relation.

In Fig. 6 the fuel flow method is applied to an airline simulated flight. Due to the higher recorded fuel flows in the ACMS data than described in the ICAO database, this results in an overestimation of thrust. Further, it is visible that the effect of airspeed is not taken into account in this method, similar to what is observed in Section 2.2.

2.4. Method 3: Gas Turbine Simulation Program (GSP)

A simulation-based approach to estimate aircraft thrust involves the Gas Turbine Simulation Program (GSP) (Nationaal Lucht- en Ruimtevaartlaboratorium, National Aerospace Lab (NLR) GSP Development Team, 2016), which is a software tool designed to calculate gas turbine performance. The GSP tool is used for high-end engine simulations to perform design studies of engine efficiency and emissions. A recent use of this GSP model is to analyse the effect of different design parameters on the climate impact of aircraft (Saluja et al., 2023). The GSP can also be used to calculate all parameters needed for engine noise calculations for more advanced aircraft noise models such as ANOPP (Gillian, 1982; Kontos et al., 1996), which can consequently be applied in noise studies to estimate the effect of changing engine parameters (Vieira et al., 2022).

For the engines of each aircraft studied in this research, GSP is used to simulate thrust for different altitudes, Mach numbers and N1 settings, as shown in Table 3. This method generated a total of 14 274 simulations for the B777-200. The simulations were performed under the international standard atmosphere (ISA) conditions at sea level, with pressure and temperature varying according to altitude in the model. The outputs of this simulation are but are not limited to, net corrected thrust, fuel flow and pressure and temperature ratios at different stages of combustion within the engine.

From this large dataset, a multi-variable linear interpolation method is used to determine the thrust level for specific flight conditions. While the GSP is modelled for ISA temperatures (15 degrees), the airline model simulations are for ISA-10 (5 degrees).

Table 3
Simulation range of GSP for different engine types.

	Altitude [m]	Mach [–]	N1%
	0–3000	0–0.6	20–104
Δ	50	0.05	5

Lower temperatures yield higher thrust under similar engine settings. This introduces an offset between the airline model and the GSP simulation. To correct for this discrepancy, a temperature correction is applied, based on the engine jet coefficients from the ANP database, as elaborated in Appendix. The resulting temperature-corrected GSP thrust profile, shown in Fig. 7, closely matches the airline model with only minor deviations.

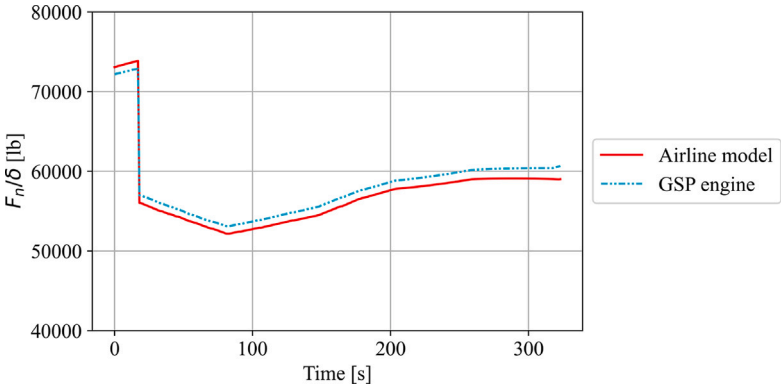

Fig. 7. Airline simulated flight of B777-200 modelled with GSP data.

2.5. Thrust input into aircraft noise modelling

Noise models are used to evaluate the amount of aircraft noise inflicted in the area around airports, with thrust being an important model input parameter. In Europe, the widely used best-practice noise model is Doc 29 (European Civil Aviation Conference, 2016b), which relies on the Noise-Power-Distance (NPD) tables providing the predicted noise level as a function of the engine's power settings (thrust) and the distance between the aircraft and the observer. The simplified representation of this model is illustrated in Fig. 8. Currently, the relationship between thrust and the expected noise level is assumed to be linear across all observation angles and distances to the ground (European Civil Aviation Conference, 2016a). An example of NPD values is given in Fig. 9 where the relation between noise, power and distance is depicted for the B777-200.

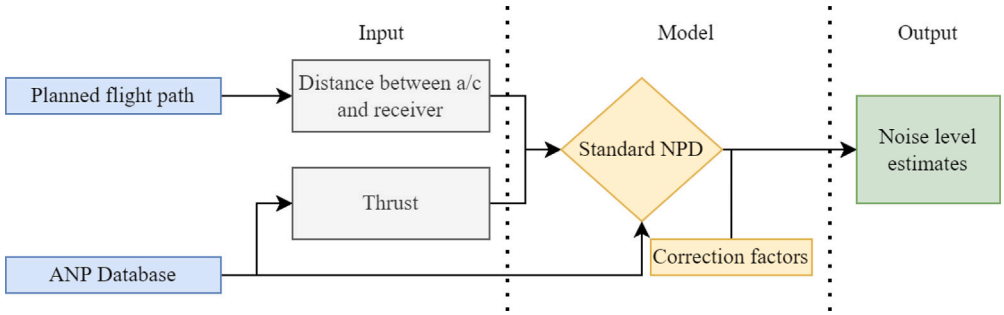

Fig. 8. Flowchart of input and output of the Doc 29 aircraft noise model.

In this paper, the Doc 29 model is used to evaluate the effect of different conversion methods on the noise predictions. This is accomplished by modelling the noise contours around Schiphol airport using the $N1\%$ data and flight paths derived from the airline-provided aircraft performance calculations. Each flight is modelled using the described methods, and the resulting differences in noise levels are categorized in different flight phases and distances from the aircraft to the ground. This categorization allows for a detailed evaluation of the accuracy of the three thrust conversion methods.

3. Results

3.1. Differences in thrust estimations using conversion methods

In this section, the above-described methods are compared to each other using two datasets. First, they are applied to the airline models' tracks to analyse the differences in N1-to-thrust conversion across the methods. The methods are then applied to actual flight

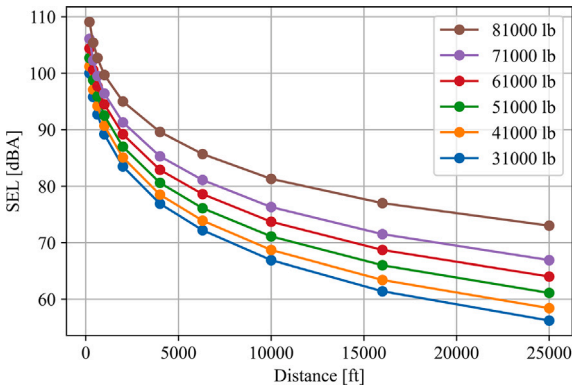

Fig. 9. The sound exposure level (SEL) as a function of distance as listed in the Noise-Power-Distance table of the B777-200. The different curves belong to the different thrust levels in the table.

data from the ACMS to assess their performance using more realistic input data. This two-step approach highlights the strengths and limitations of each method in different contexts.

3.1.1. Airline-provided aircraft performance calculations

The thrust is modelled using the three methods for seven different take-off weights. A typical example of the results for a flight with maximum take-off weight is presented in Fig. 10. Considering the airline model as a reference, Fig. 11 illustrates the average deviations and the corresponding standard deviations (calculated across the seven take-off weights) as a function of altitude. The right axis depicts the deviation as a percentage of the maximum flat rated thrust at mean sea level. A few observations are highlighted.

The first method, the ANP relation, gives stable results when looking at the different departures, indicated by a very small standard deviation. Furthermore, it is visible that the discrepancies in thrust relative to the airline model grow over altitude. This is likely because, for this aircraft, the coefficients F_0, G_A and G_B are set to 0. As a result, the effects of speed and altitude on thrust are not accounted for in the calculations.

The second method, which uses the fuel flow, exhibits a similar trend of increasing thrust over time as observed with the ANP relation. However, during the development of this method, the effect of speed is not considered in the relation. This method has a large, although constant, standard deviation when comparing different take-off weight departures.

Finally, the third method, using the GSP database, gives the best result with only a small, but constant, offset. It shows a good approximation of the climb phase and thus altitude, speed and temperature have been compensated for in the modelling.

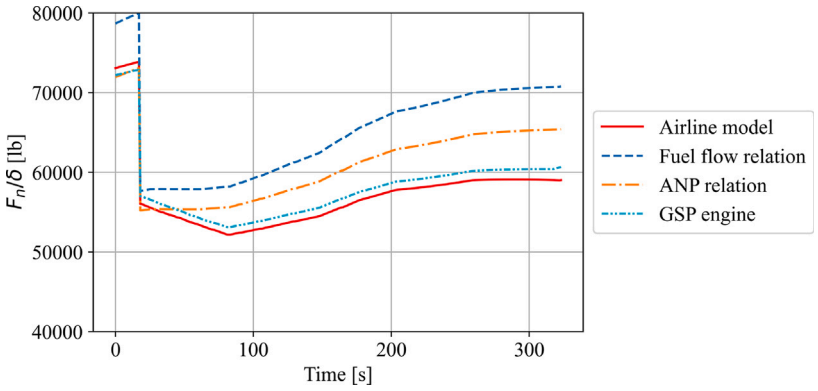

Fig. 10. Example of the airline model flight thrust profile of the B777-200 derived from N1% using three conversion methods.

3.1.2. Aircraft condition and monitoring system

The above-described methods are also applied to real flight data from the ACMS. This analysis aims to evaluate how the methods perform under different scenarios than a consistent ISA standard departure. Using the ACMS, parameters such as position, speed and N1% are taken and thrust is calculated using the same methods described earlier. The results are presented in Fig. 12. In this figure, the thrust estimations from the three methods are presented, each based on the same input information (height, speed and N1%). As can be observed, the actually followed thrust pattern shows more rapid fluctuations. This time, there is no golden truth to compare these methods with.

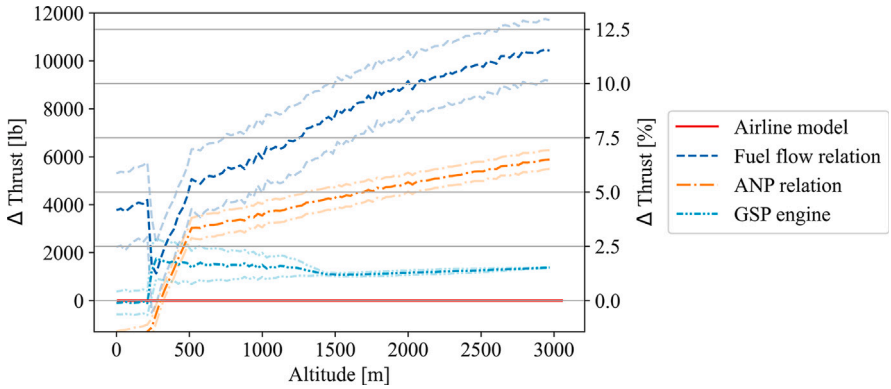

Fig. 11. Average deviation and standard deviation of thrust compared to the airline model of 7 different take-off weights of the B777-200.

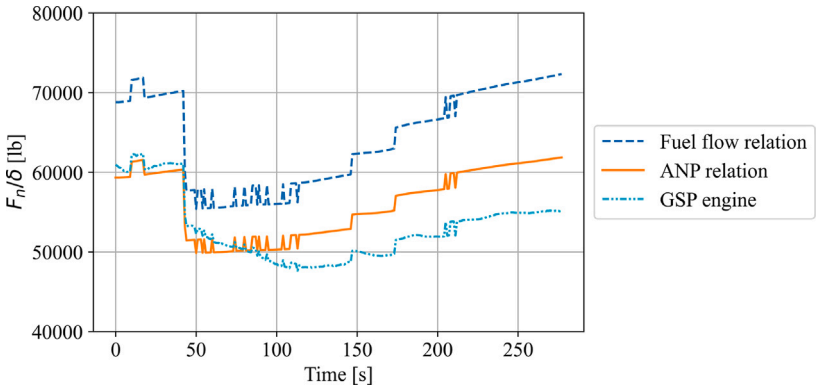

Fig. 12. ACMS flight data of the B777-200 converted into thrust using three conversion methods.

The sharp peaks in the figure are caused by an inconsistent $N1\%$, switching between for example 88% and 89%. Apart from these variations, a similar pattern is visible in this procedure as to the airline model, where the first 50 s correspond to a take-off, followed by a cut-back and a climb-out phase. Both the ANP and fuel flow methods show a flatter curve during the acceleration phase (60–120 s) and a strong growing thrust during the climb phase. These methods however do not fully account for atmospheric effects or changing speed. In contrast, the GSP method shows a decrease in thrust during acceleration and a more nuanced curve with growing altitude. Again, the fuel flow method produces the highest thrust estimates, while the GSP shows the lowest estimates.

For a different aircraft type, the A330-300, the three methods exhibit similar behaviour, presented in Fig. 13. Contrary to the B777-200, the ANP relation for this aircraft includes non-zero coefficients for F_0 and G_A, which results in a thrust estimation that includes speed and altitude. The GSP thrust estimation is again lower than the ANP but follows a comparable pattern. The fuel flow method, depicted in dark blue, produces a higher thrust estimation than the ANP, although with a significantly smaller absolute offset than for the B777-200.

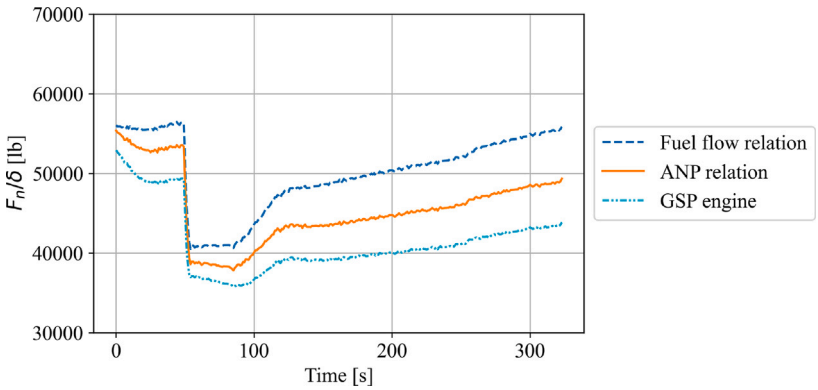

Fig. 13. ACMS flight data of the A330-300 converted into thrust using three conversion methods.

3.2. Effect of thrust models on noise contours

The calculated thrust is now used for noise modelling. The most common output of noise models is a contour of expected noise levels in dBA. For this research, Sound Exposure Levels (SEL) are modelled for a grid size of about 25 by 30 km for a single departing flight. As mentioned in Section 2.1, the airline model is considered the most reliable and is therefore used as a baseline for comparing the different noise contours. Fig. 14 illustrates the expected noise levels for a B777-200 departure. The departure runway 24/06 is highlighted in green and the orange triangle indicates the location of the air traffic control tower (0,0).

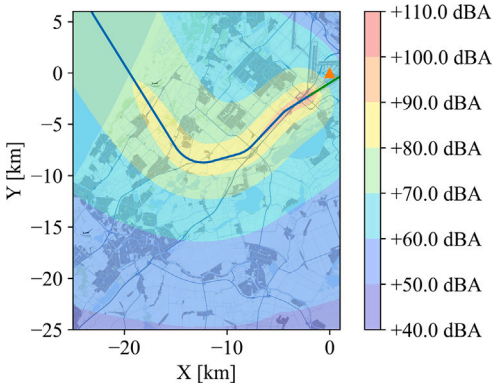

Fig. 14. SEL contour of a single departure operation of the B777-200 using the airline modelled thrust data.

Noise contours for the three methods were generated, and their differences with the baseline are presented in Fig. 15. Negative values (blue colour) in these figures indicate that the predicted noise levels are lower than the baseline level. The noise contours resulting from using the ANP relation, visible in Fig. 15(d), reveals a slight underestimation of the noise over the start area up to 0.5 dBA difference. This is expected as the thrust estimated during the initial take-off is lower than that predicted by the airline model. This increases to a maximum of 1.8 dBA overestimation in later flight phases. Fig. 15(e) shows the differences between the baseline and fuel flow method. These differences are much larger, about 3 dBA maximum, mostly in the later flight phases. This highlights the effect of the overestimated thrust in the fuel flow model. Finally, Fig. 15(f) illustrates the differences in noise contour between the baseline and the GSP-modelled thrust. This method shows a slight underestimation of 0.4 dBA in high-noise areas and an overestimation of 0.3 dBA in low-noise areas (beyond a 10 km slant range).

4. Estimation of new ANP parameters

The previous sections highlight that the ANP relation is a promising and straightforward method for N1-to-thrust conversion, as it captures the main influencing parameters affecting this conversion. However, the necessary engine parameters (E_0 to K_4) are not available for most aircraft. From Section 3.2, it is evident that the GSP also takes all influencing parameters into account and provides thrust estimates that are in good agreement with those of the airline model, although with a higher computational burden. In this section, new ANP coefficients are estimated from the large GSP dataset using the least squares methods. This is useful to expand the current ANP database with new or updated aircraft types.

4.1. Two least-squares-based methods

When looking at the existing coefficients in the ANP database for different aircraft types, a few observations can be made. For example, the speed coefficient F_0 is always negative, as is the temperature coefficient H. This aligns with physical principles as, for example, thrust decreases with increasing temperature (Deiler, 2023). To estimate the seven engine parameters (as provided in the ANP database) from the GSP data, two least-squares-based methods, namely (unbounded) least squares (LS) and bounded least squares (BLS) are used. A BLS approach is chosen to incorporate prior information by setting lower and upper bounds on certain parameters, ensuring they remain within their expected ranges. The BLS method used in this paper utilizes a generalized optimization algorithm based on a non-negative least squares (NNLS) problem used in Amiri-Simkooei (2016).

Table 4 shows the original ANP coefficients, together with the coefficients estimated from GSP data. These coefficients are estimated from the GSP dataset prior to the temperature correction (Appendix). The second row shows the results of the LS method. Contrary to what is expected, H is a large positive number, while E_0 is fairly small. When approximating a model with least-squares, the model residuals $\hat{e}$ are minimized. However, prior information about physical principles shows that there is a negative correlation between temperature and thrust, thus the smallest $\hat{e}$ does not necessarily provide realistic results. If H is bound to be negative (i.e. less than 0), the results change to the coefficients provided in the third row using the BLS method. Not only do the values for H and E_0 change but the coefficient G_A also changes. This is because temperature decreases with altitude and these parameters are thus not fully independent variables. The estimated correlation coefficient ρ between the two parameters H and G_A is close to one

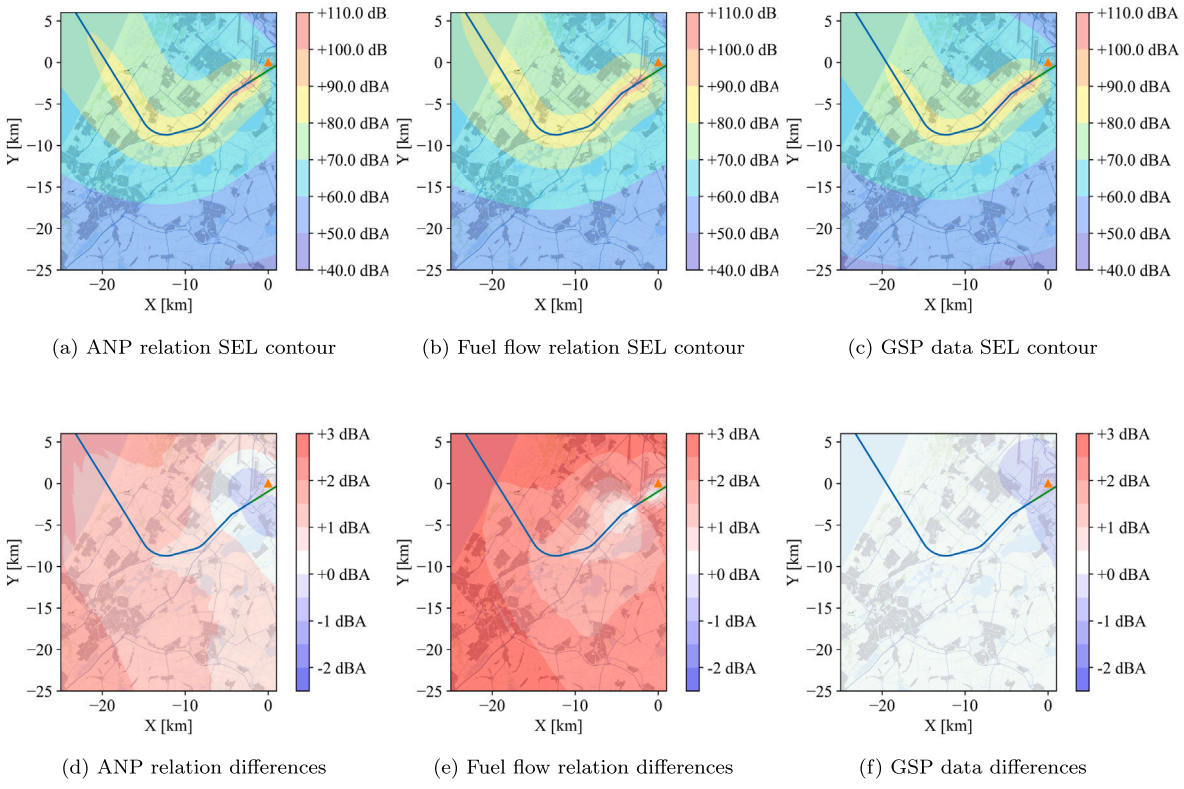

(a) ANP relation SEL contour (b) Fuel flow relation SEL contour (c) GSP data SEL contour

(d) ANP relation differences (e) Fuel flow relation differences (f) GSP data differences

Fig. 15. Noise contours of the differences between three calculation methods with the airline model for B777-200.

Table 4
Old and new ANP coefficients of the B777-200.

Method	E_0	F_0	G_A	G_B	H	K_3	K_4
ANP	32710	0	0	0	0	−1258	16.16
LS	7825	−69.51	1.608	1.46e−06	921.6	−654.2	12.49
Bounded LS	22124	−69.51	−0.2805	1.46e−06	−31.67	−654.2	12.49

for this dataset ($\rho = 0.999$). This indicates that these two LS estimates can interchangeably be affected by each other while resulting in the same LS fit (very similar $\hat{e}$). This is, however, only the case for modelling within the range of the GSP dataset.

Applying all above-estimated coefficients to an airline-modelled flight yields the results shown in Fig. 16. Although the differences in $\hat{e}$ between the LS- and BLS-estimated coefficients are small, they give rise to significantly different results for the estimated

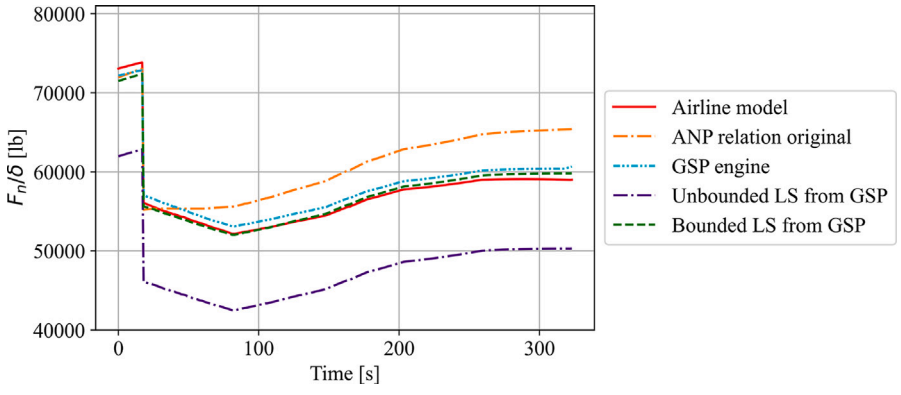

Fig. 16. Airline simulated flight modelled with different ANP coefficients for B777-200.

Table 5
New ANP coefficients of the B777-200 obtained from GSP and airline data and the relative change with respect to the BLS.

Method	E_0	F_0	G_A	G_B	H	K_3	K_4
LS from GSP+	22 041	−69.53	−0.272	1.55e−06	−25.34	−654.0	12.49
Relative change from BLS	−83	−0.02	0.0085	−1.4e−05	6.33	0.2	0

parameters. The LS-based relation exhibits a large negative offset compared to the GSP results, whereas the BLS estimation shows only a small offset. This highlights the improved alignment of the BLS coefficients with the modelled thrust profiles.

To further explain the differences observed between the two least-squares methods and the GSP results, a detailed analysis was conducted. From the analysis, it became clear that the discrepancies can be attributed to the atmospheric simulation ranges. As noted in Section 2.4, there is a 10-degree temperature difference between the GSP dataset and the airline model. As there is no independent temperature variable in the GSP dataset, the interrelated impact of the height G_a and temperature H variables on the thrust is estimated simultaneously during the LS. This interrelation can have a significant impact on the estimated parameters, and in fact, the primary reason for the differences between LS and BLS as illustrated in Fig. 16. When the LS and BLS methods were applied to a flight under ISA conditions, the results showed no significant discrepancies between the two methods, with only limited deviation (<300 lb) from the GSP method.

To adopt a more conservative approach and mitigate the impact of the high correlation between G_a and H on the parameter estimation, BLS is preferable over the LS method. By incorporating physical principles, BLS can better account for the interdependent variations of these highly correlated variables. Conversely, by expanding the dataset to include a broader range for both temperatures and altitudes, this linear dependency (correlation) can be reduced. This reduction in correlation would consequently result in more accurate and realistic estimates of the two parameters when using the LS method.

To validate the BLS estimated temperature coefficient H, the GSP dataset is expanded with an additional flight example from the airline model (GSP+). Since the dataset now includes data from two different atmospheric conditions, the LS method is expected to provide a better estimate of the temperature effect on the thrust. The new ANP coefficients were subsequently estimated through the unbounded LS method (Table 5). Although the resulting values are slightly different from the BLS results, the thrust estimation, depicted in Fig. 17, is quite similar. This indicates that while the GSP dataset can provide useful insights into thrust relations, it is important to validate the results with either physical principles or additional data that extend beyond the limited range of conditions present in the original dataset. Nevertheless, the results obtained using BLS provide promising initial outcomes and will serve as a foundation for further research in this study. In conclusion, these findings demonstrate that BLS can accurately estimate the temperature effect on thrust, aligning closely with the temperature correction applied to the GSP dataset.

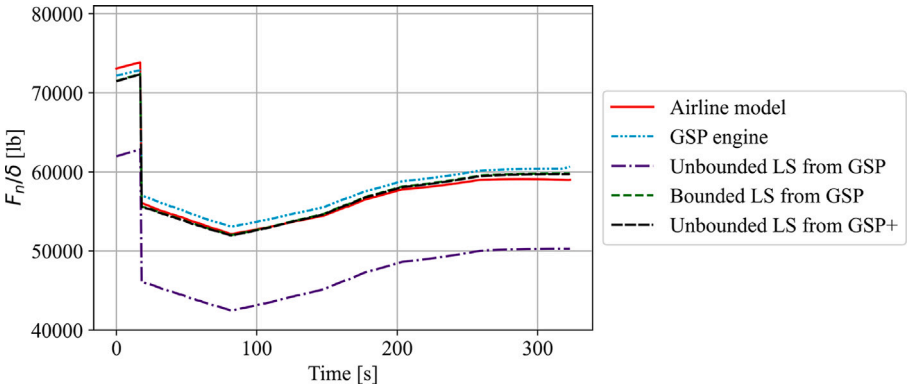

Fig. 17. B777-200 simulated flight modelled with ANP for different LS methods.

In Fig. 18, the differences in thrust estimation using the new method compared to the airline model are visualized across all seven take-off weights. The results indicate that not only is the difference between thrust estimation minimal, but it is also consistent over all flights. The impact of these differences on the noise contour is illustrated in Fig. 19, resulting in a maximum deviation of less than 0.6 dBA. Given that such a deviation is practically negligible, the proposed method is considered reliable and suitable for this application.

4.2. Checking validity of the method for the B737-800

The benefit of the proposed method is that it enables the estimation of the ANP coefficients for all aircraft. This gives the opportunity to expand the current ANP database with newer aircraft types or with aircraft that are currently missing from the database. For example, one of the most common aircraft at Schiphol Airport, the B737-800, is used here for testing, as both the airline model and GSP data are available for this aircraft. It is important to note that B737-800 is an older model, and the resulting airline-provided aircraft performance calculations are also based on an older version. This might introduce slight discrepancies in

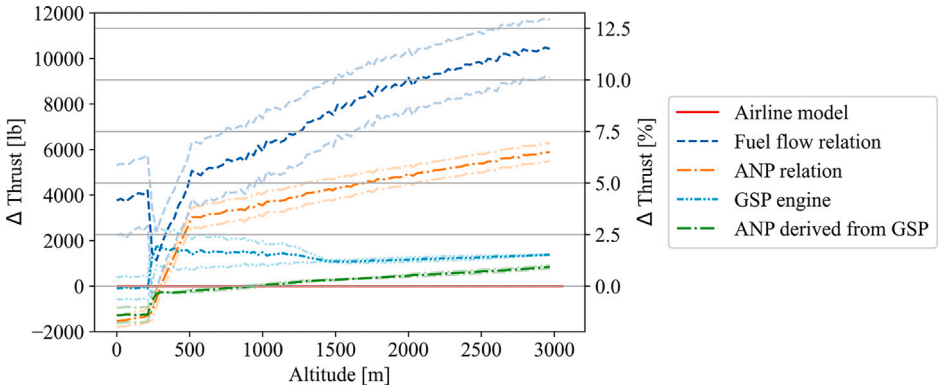

Fig. 18. Average deviation and standard deviation of thrust estimations compared to the airline model of 7 different take-off weights of the B777-200.

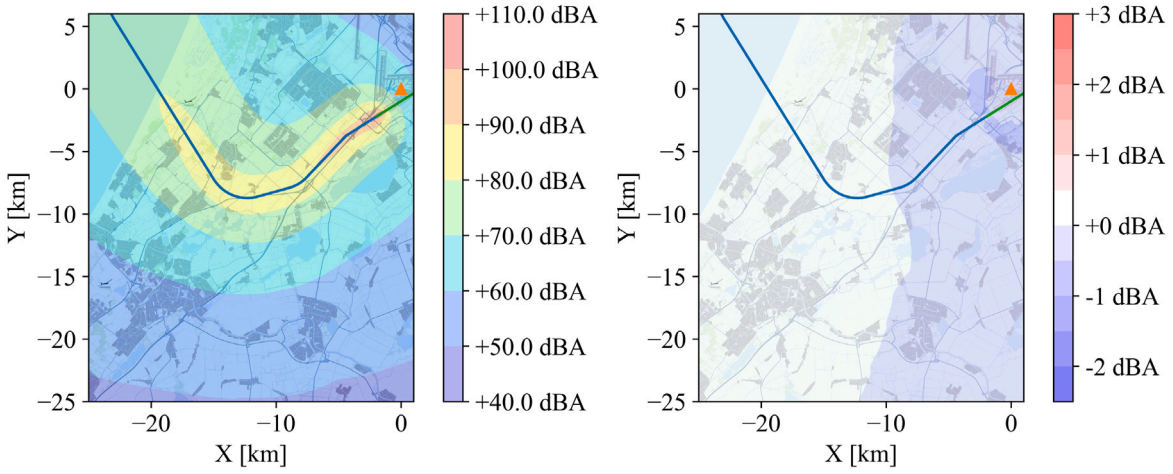

(a) SEL contour (b) Noise contour of the differences.

Fig. 19. Noise contour of the new BLS-derived ANP method and the differences with the airline model for the B777-200.

Table 6
New ANP coefficients of the B737-800 derived from GSP data.

Method	E_0	F_0	G_A	G_B	H	K_3	K_4
Least-squares	1919	−15.77	0.376	3.68e−07	216.8	−172.5	3.661
Bounded LS	5260	−15.77	−0.0653	3.68e−07	−5.934	−172.5	3.661

the results. The estimated LS and BLS coefficients are presented in Table 6, and an example flight is visualized in Fig. 20. The differences in thrust estimation for the three different take-off weights are given in Fig. 21.

For the B737-800, similar results are found as for the B777-200. The GSP method slightly overestimates the thrust compared to the airline model. The LS approximation gives a high value for H and hence underestimates the thrust. When H is constrained to be negative, the new BLS produces a more accurate thrust estimate, closely following the airline model. This outcome was further validated by expanding the GSP dataset with an airline-modelled flight. Applying the LS or BLS method to this expanded data gave (again) similar results to the BLS values presented in Table 6.

While this method has been validated using the B737-800, further validation would benefit the inclusion of a broader range of aircraft types. Additionally, a notable limitation of this study is the limited number of flights within the dataset. This constraint could be addressed by extending the research to include a variety of take-off procedures and diverse weather conditions.

The resulting noise contours for the two methods are presented in Fig. 22, providing quite similar results with the airline model. The GSP-based contour exhibits differences ranging from 0 to 1.2 dBA, mainly due to the higher estimated thrust after acceleration. The BLS-derived noise contour, shown on the right, also closely matches the airline model, though with minor deviations: a slight underestimation during take-off (−0.3 dBA), and an overestimation of up to 1.3 dBA in later flight phases.

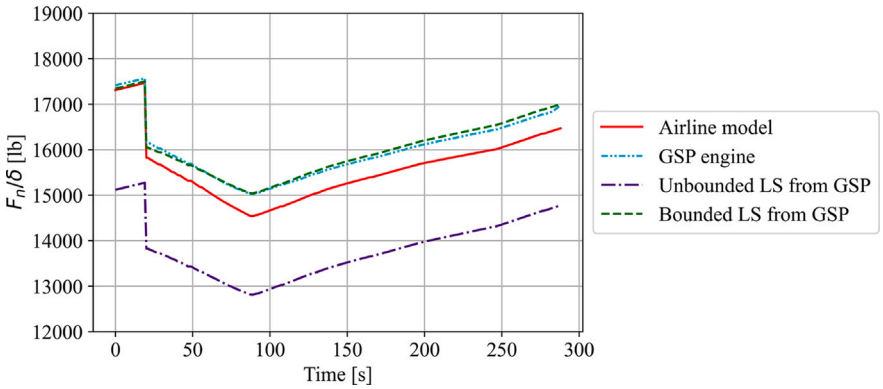

Fig. 20. Example flight of the B737-800 with GSP and GSP derived thrust estimation compared to the airline model.

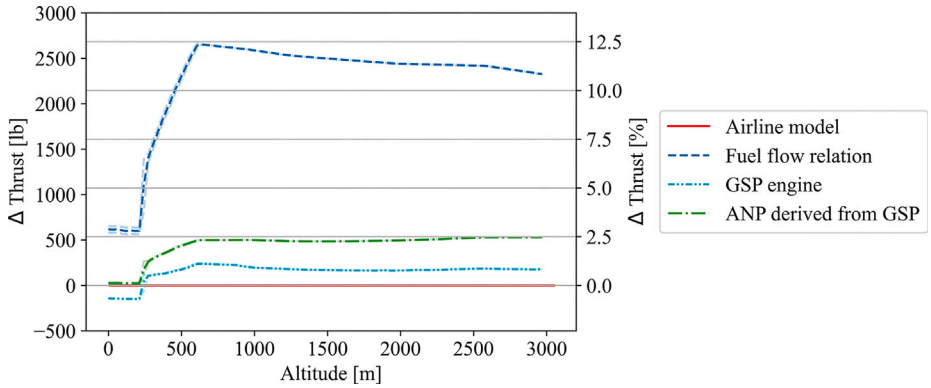

Fig. 21. Average deviation and standard deviation of thrust compared to airline model of 3 different take-off weights of the B737-800.

5. Conclusions

This paper assesses different methods of estimating thrust of departing aircraft and their effect on noise modelling. For the methods investigated, the approach is to calculate aircraft thrust from the engine's rotational speed N1. The estimates are validated with airline-provided aircraft performance calculations. The first method is the best-practice method from the Aircraft Noise and Performance (ANP) database. For a second method, a relation was established between thrust and the fuel flow to the engines gathered from Aircraft Condition and Monitoring System (ACMS) data. This method is fully empirical and thus significantly different from the previous methods. The final method is based on the Gas Turbine Simulation Program (GSP). The three methods were then used to find thrust input to the Doc.29 noise model to compare their thrust profiles and corresponding noise footprint.

The current best-practice method approximates the thrust well but currently has a limited range of aircraft types for which it can be applied. The fuel flow method gives good insight into actual flight data and the important parameters for thrust estimation but shows large deviations from the airline model. The GSP method is found to provide a good approximation of the thrust. The effect of these different methods on the noise predictions was up to 3 dBA in departures. To improve the performance of the current best practice methods, the advantages of the above methods were combined. New engine coefficients were estimated from the GSP database with bounded least-squares and implemented into the ANP method. Although the updated results still showed differences with the GSP method, it is more accurate than current best-practice models.

In conclusion, this paper gives insight into the advantages and disadvantages of the different thrust estimation methods and their effect on aircraft noise estimations. A very important result is that methodologies such as GSP can be used to derive coefficients for determining thrust, accounting for the N1, fully in line with those currently used in the ANP database. Despite the computational requirements, this approach is cheap compared to real engine tests. In addition, it can easily account for new engine types and for the full range of engine types currently used by expanding the current ANP database. However, the limitation of available validation data for public use remains a challenge. Using this new method is a step towards better aircraft noise modelling and inevitably better flight planning.

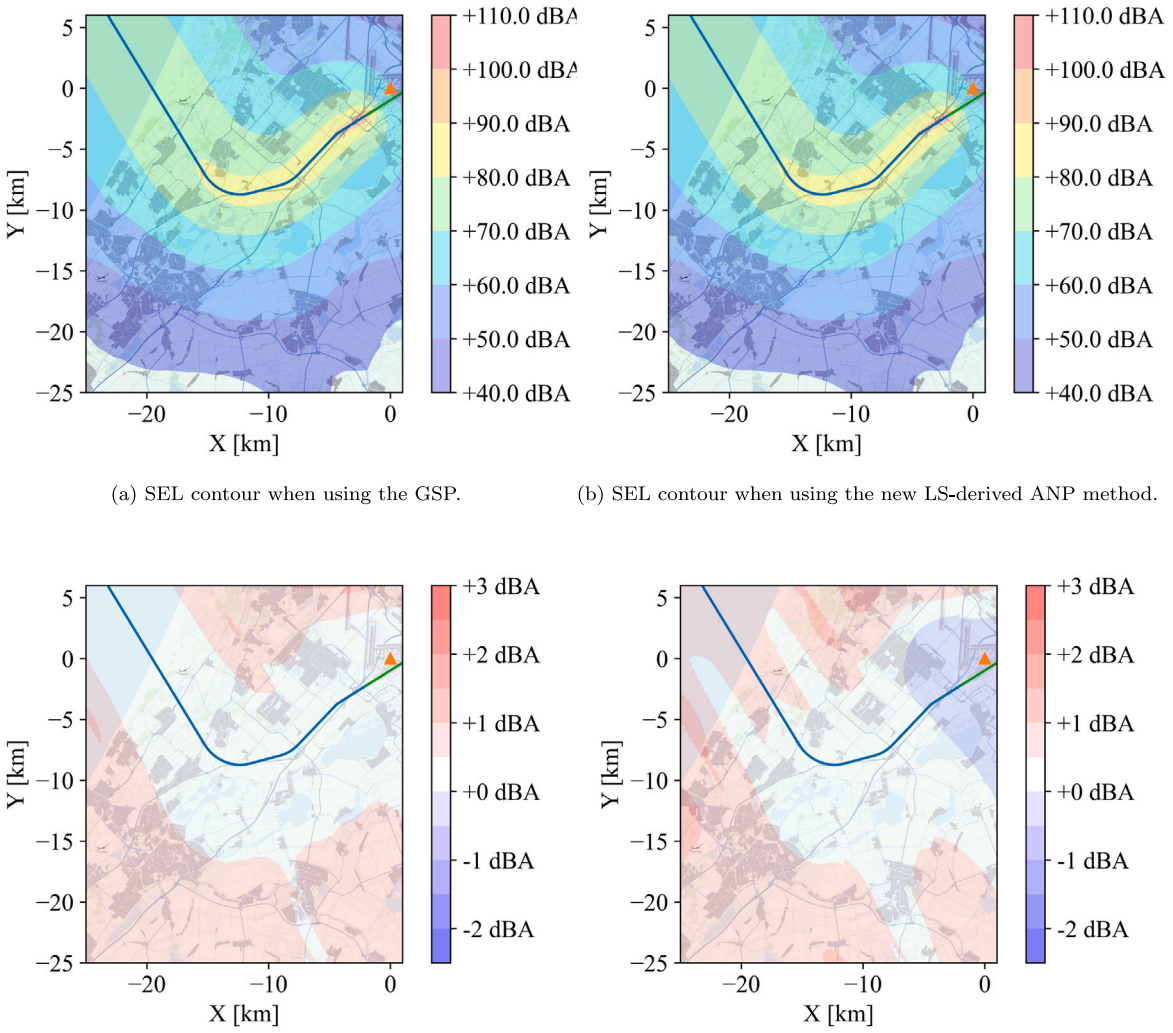

(a) SEL contour when using the GSP.

(b) SEL contour when using the new LS-derived ANP method.

(c) Differences in calculated noise contour when using the GSP.

(d) Differences in calculated noise contour when using the new LS-derived ANP method.

Fig. 22. Noise contours of the differences between multiple calculation methods with the airline model for the B737-800.

CRediT authorship contribution statement

Rebekka C. van der Grift: Writing – original draft, Visualization, Validation, Software, Resources, Methodology, Formal analysis, Data curation, Conceptualization. **Mirjam Snellen:** Writing – review & editing, Supervision, Methodology, Conceptualization. **Alireza Amiri-Simkooei:** Writing – review & editing, Writing – original draft, Validation, Supervision, Methodology, Conceptualization.

Acknowledgements

This work was mainly supported by the Knowledge and Development Centre (KDC) Mainport Schiphol. The authors are also grateful to the EC for supporting the present work, partly performed within the NEEDED project, funded by the European Union's Horizon Europe research and innovation programme under grant agreement no. 101095754 (NEEDED). This publication solely reflects the authors' view and neither the European Union, nor the funding Agencies can be held responsible for the information it contains.

Appendix. Temperature correction for GSP

The Gas turbine Simulation Program (GSP) is run under specific atmospheric conditions and a large range of operating parameters. The current dataset from this simulation is set to ISA conditions. As the flight data used in this paper operates under different temperatures (ISA-10), a thrust correction is needed after the interpolation from the GSP dataset.

As mentioned in Section 2.2, the jet engine coefficients are given by procedural step for most aircraft types in the ANP database. The temperature coefficients H are analysed to estimate the effect of temperature on the produced thrust. For this, only non-zero values for H during the climb-out step are used as used in Eq. (1). These values are plotted against the maximum sea level static thrust as reported for that aircraft type. A fit with a slope of -0.0050533 C°/lb/$F_{n,max}$ is found which is shown in Fig. A.23. Although variation is visible in this plot, the fit shows a good correlation and p-value. The benefit of this general correction factor is that it applies to all the different aircraft types covered in this paper.

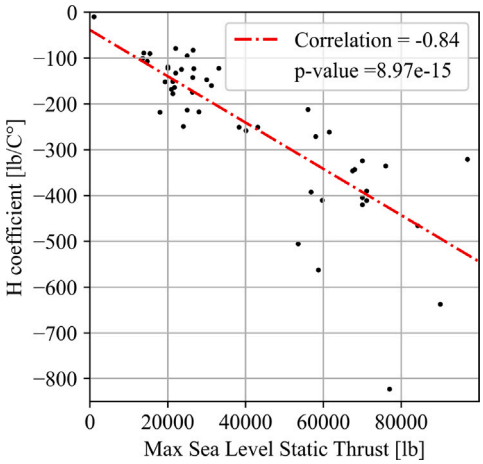

Fig. A.23. Fit of temperature coefficient H based on maximum sea level static thrust.

The found correction is applied to the GSP thrust estimation for the flights presented in this paper. This results in a shift of about 3800 lb as can be seen in Fig. A.24.

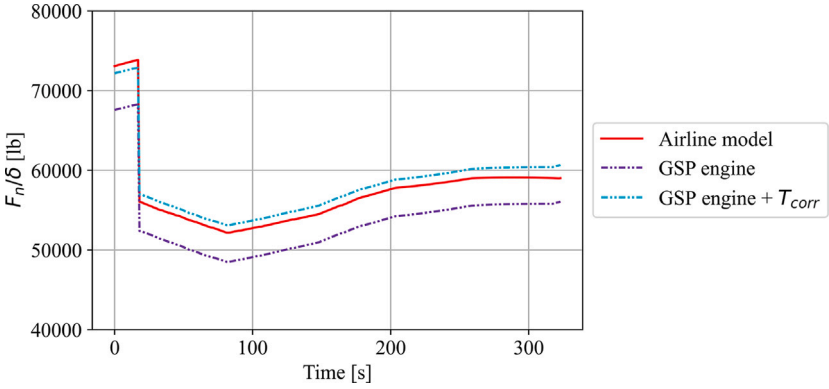

Fig. A.24. Effect of temperature correction on the GSP thrust estimation.

References

Amiri-Simkooei, A.R., 2016. Non-negative least-squares variance component estimation with application to GPS time series. J. Geod. 90, 451–466. http://dx.doi.org/10.1007/S00190-016-0886-9/TABLES/2.

Anna, L., Blangiardo, M., Fortunato, L., Floud, S., Hoogh, K.D., Fecht, D., Ghosh, R.E., Laszlo, H.E., Pearson, C., Beale, L., Beevers, S., Gulliver, J., Best, N., Richardson, S., Elliott, P., 2013. Aircraft noise and cardiovascular disease near heathrow airport in London: small area study. BMJ 347, http://dx.doi.org/10.1136/BMJ.F5432.

Basner, M., McGuire, S., 2018. WHO environmental noise guidelines for the European region: A systematic review on environmental noise and effects on sleep. Int. J. Environ. Res. Public Heal. 15 (3), http://dx.doi.org/10.3390/ijerph15030519.

Behere, A., Lim, D., Li, Y., Jin, Y.C., Gao, Z., Kirby, M., Mavris, D., 2020. Sensitivity analysis of airport level environmental impacts to aircraft thrust, weight, and departure procedures. AIAA Scitech Forum http://dx.doi.org/10.2514/6.2020-1731.

Bensel, A., Scholz, D., 2018. Characteristics of the specific fuel consumption for jet engines. http://dx.doi.org/10.15488/4316.
Boeing 747 Performance Engineers Manual, 1989. 747-400/CF6-80C2B1F. p. 7.29, 4-LA02 ed.
Chati, Y.S., Balakrishnan, H., 2014. Analysis of aircraft fuel burn and emissions in the landing and take off cycle using operational data. In: 6th International Conference on Research in Air Transportation. ICRAT.
Deiler, C., 2023. Engine thrust model determination and analysis using a large operational flight database. CEAS Aeronaut. J. 3, 29–45. http://dx.doi.org/10.1007/s13272-022-00625-y.
DuBois, D., Paynter, G.C., 2006. "Fuel flow method2" for estimating aircraft emission. J. Aerosp. 115, 1–14, URL: https://www.jstor.org/stable/pdf/44657657.pdf.
European Civil Aviation Conference, 2016a. CEAC Doc 29 on Standard Method of Computing Noise Contours around Civil Airports, 4th Edition Report, Volume 2: Technical Guide. Technical Report, ECAC.CEAC Doc29, Neuilly-sur-Seine Cedex, France.
European Civil Aviation Conference, 2016b. Doc 29 Report on Standard Method of Computing Noise Contours around Civil Airports, 4th Edition, Volume 1: Applications Guide. Technical Report, ECAC.CEAC Doc29, Neuilly-sur-Seine Cedex, France.
European Union Aviation Safety Agency, 2024. Aircraft noise and performance (ANP) data. https://www.easa.europa.eu/en/domains/environment/policy-support-and-research/aircraft-noise-and-performance-anp-data. (Accessed 29 October 2024).
European Union Aviation Safety Agency, 2025. ICAO aircraft engine emissions databank. https://www.easa.europa.eu/en/domains/environment/icao-aircraft-engine-emissions-databank. (Accessed 29 January 2025).
Gillian, R.E., 1982. Aircraft noise prediction program user's manual.
Kontos, K.B., Janardan, B.A., Gliebe, P.R., 1996. Improved NASA-ANOPP noise prediction computer code for advanced subsonic propulsion systems.
Linke-Diesinger, A., 2008. Systems of Commercial Turbofan Engines: An Introduction to Systems Functions. Springer, Hamburg, Germany.
Meister, J., 2024. Power setting estimation of departing civil jet aircraft based on machine learning. J. Aircr. 61, 1195–1204. http://dx.doi.org/10.2514/1.C037619.
Meister, J., Schalcher, S., Wunderli, J.-M., Jäger, D., Zellmann, C., Schäffer, B., Sescu, A., 2021. Comparison of the aircraft noise calculation programs sonAIR, FLULA2 and AEDT with noise measurements of single flights. Aerospace 8, http://dx.doi.org/10.3390/aerospace8120388.
Merino-Martínez, R., Heblij, S.J., Bergmans, D.H.T., Snellen, M., Simons, D.G., 2018. Improving aircraft noise predictions considering fan rotational speed. J. Aircr. 56, http://dx.doi.org/10.2514/1.C034849.
Nationaal Lucht- en Ruimtevaartlaboratorium, National Aerospace Lab (NLR) GSP Development Team, 2016. GSP user manual.
Patterson, J., Noel, G.J., Senzig, D.A., Roof, C.J., Fleming, G.G., 2009. Analysis of departure and arrival profiles using real-time aircraft data. J. Aircr. 46, 1094–1103. http://dx.doi.org/10.2514/1.42432.
Poles, D., 2009. Base of Aircraft Data (BADA) Aircraft Performance Modelling Report. Technical Report EEC Technical/Scientific Report No. 2009-09, EUROCONTROL.
Pretto, M., Dorbolò, L., Giannattasio, P., Zanon, A., 2024. Aircraft operation reconstruction and airport noise prediction from high-resolution flight tracking data. Transp. Res. Part D: Transp. Environ. 135, 104397. http://dx.doi.org/10.1016/J.TRD.2024.104397.
Pretto, M., Giannattasio, P., Gennaro, M.D., 2022. Mixed analysis-synthesis approach for estimating airport noise from civil air traffic. Transp. Res. Part D: Transp. Environ. 106, 103248. http://dx.doi.org/10.1016/J.TRD.2022.103248.
Ramseier, T., Pieren, R., 2024. Estimation of the fan rotational speed using flyover audio recordings. J. Aircr. 61, 58–72. http://dx.doi.org/10.2514/1.C037371.
Saluja, H.S., Yin, F., Rao, A.G., Grewe, V., 2023. Effect of engine design parameters on the climate impact of aircraft: A case study based on short-medium range mission. Aerosp. 10, 1004. http://dx.doi.org/10.3390/AEROSPACE10121004, 2023, Vol. 10, Page 1004.
Schäfer, M., Strohmeier, M., Lenders, V., Martinovic, I., Wilhelm, M., 2014. Bringing up OpenSky: A large-scale ADS-B sensor network for research. In: IPSN 2014 - Proceedings of the 13th International Symposium on Information Processing in Sensor Networks (Part of CPS Week). IEEE Computer Society, pp. 83–94. http://dx.doi.org/10.1109/IPSN.2014.6846743.
Struempfel, C., Hübner, J., 2020. Aircraft noise modeling of departure flight events based on radar tracks and actual aircraft performance parameters. In: Proceedings of DAGA 2020 46. Jahrestagung für Akustik. Technische Universität Berlin, Hannover, URL: https://www.researchgate.net/publication/340461180.
Sun, J., Ellerbroek, J., Hoekstra, J.M., 2018. Aircraft initial mass estimation using Bayesian inference method. Transp. Res. Part C: Emerg. Technol. 90, 59–73. http://dx.doi.org/10.1016/j.trc.2018.02.022.
Sun, J., Hoekstra, J.M., Ellerbroek, J., 2020. OpenAP: An open-source aircraft performance model for air transportation studies and simulations. Aerospace 7 (8), 104.
Vieira, A., von den Hoff, B., Snellen, M., Simons, D.G., 2022. Comparison of semi-empirical noise models with flyover measurements of operating aircraft. J. Aircr. 1–14. http://dx.doi.org/10.2514/1.C036387.
Zellmann, C., Schäffer, B., Wunderli, J.M., 2018. Aircraft noise emission model accounting for aircraft flight parameters. J. Aircr. 55, 682–695. http://dx.doi.org/10.2514/1.C034275.